The influence of underlying metals on the hydrogen evolution from plasma-deposited silicon nitride films

Takamaro Kikkawa and Nobuhiro Endo

Citation: Journal of Applied Physics **71**, 958 (1992); doi: 10.1063/1.351321
View online: http://dx.doi.org/10.1063/1.351321
View Table of Contents: http://scitation.aip.org/content/aip/journal/jap/71/2?ver=pdfcov
Published by the AIP Publishing

The influence of underlying metals on the hydrogen evolution from plasma-deposited silicon nitride films

Takamaro Kikkawa and Nobuhiro Endo
Microelectronics Research Laboratories, NEC Corporation, 1120 Shimokuzawa, Sagamihara City, 229 Japan

(Received 24 May 1991; accepted for publication 11 October 1991)

The influence of underlying metals on hydrogen evolution from plasma-enhanced chemical vapor deposited silicon nitride (*P*-SiN) films was investigated. Titanium (Ti), tungsten (W), and tungsten silicide (WSi_x:$x=2.3$) cap layers were deposited onto pure-Al, Al-1%Si, Al-0.5%Cu and Al-1%Si-0.5%Cu films on oxidized silicon wafers. The bilayers and Al-alloys were covered with *P*-SiN films and heated. It was found that the hydrogen evolution rates for the *P*-SiN films were influenced by the underlying bilayers as well as Al-alloys. Copper (Cu) addition to underlying Al films raised the hydrogen evolution rate peak temperature for the cover *P*-SiN film, due to the suppression of cover *P*-SiN film blistering and cracking as a result of Al-Cu hardening. Titanium thin-film capping on the Al-alloy also raised the hydrogen evolution rate peak temperature for the *P*-SiN film, as results of Ti adhesive layer and thermally stable intermetallic compound formation, $TiAl_3$.

I. INTRODUCTION

One of the most important problems in very large scale integrated circuit (VLSI) metallization involves open failures in aluminum (Al) conductors, caused by so-called stress-induced migration of Al atoms during heat treatments.[1–13] The use of plasma-enhanced chemical vapor deposited silicon nitride (*P*-SiN) films has caused voids in underlying Al films during both low-temperature (<250 °C) aging tests[1–7] and high-temperature (>450 °C) wafer processing.[8–13] It has been reported that compressive stresses in cover films cause voids in Al films.[2,3] The cover film may also act as a volume constraint for Al lines.[4] The thermal expansion mismatch between Al and an underlying Si substrate might cause voids.[3–5] Gaseous contamination during sputtering has also been reported as a cause of intergranular void formation in Al.[6,7] However, only a few studies have been made in terms of hydrogen in *P*-SiN films deposited on Al films.[8–10] We have previously reported that underlying Al deformation occurred during heat treatment due to the cover *P*-SiN film blistering and hydrogen accumulation[8] and that Ti thin-film capping on Al conductors could prevent Al deformation.[11]

The present study was made to investigate the influence of underlying metals on the hydrogen evolution from the cover *P*-SiN films. This paper reports that the hydrogen evolution rates for the *P*-SiN film were influenced by the underlying materials.

II. EXPERIMENT

Pure-Al, Al-1%Si, Al-0.5%Cu, and Al-1%Si-0.5%Cu films were deposited by direct current (dc) magnetron sputtering onto oxidized 4-in. (100) Si substrates. The Al films were 0.5 μm thick. Titanium (Ti), tungsten (W), and silicon-rich tungsten silicide (WSi_x:$x=2.3$), 0.1 μm thick, were deposited separately onto the Al-alloy films using the same dc sputtering system. The bilayer metal as well as Al-alloy films were covered with 1.0-μm-thick *P*-SiN films, which were deposited by dissociation of a mixture of NH_3 and SiH_4 gases at 320 °C, using a plasma-enhanced chemical vapor deposition (PECVD) reactor.

The hydrogen evolution rate for *P*-SiN films, as a function of temperature, is proportional to the amount of detected current by a quadrupole mass spectrometer. When the heating rate is 200 °C/h (3.3 °C/min), the detection current of 2×10^{-10} A for H_2 is equivalent to the hydrogen evolution rate of 2.5×10^{-3} ml/min. The temperature dependence of the hydrogen evolution rate was measured by assembled apparatus comprised of a small furnace with provisions for temperature monitoring and control, a quadrupole mass spectrometer, and a diffusion pump capable of achieving pressure reduction down to 1.3×10^{-5} Pa. In this experiment, the temperature was stepped up, at a 5 °C/min rate, to 800 °C.

Film stresses as a function of temperature were calculated from the wafer curvature measured *in situ* by a laser based optical shift measurement technique during thermal cycling in a nitrogen ambient using halogen lamp heating. The heating and cooling rates were 5 °C/min. The effective stress for the layered film is defined as an overall stress for the layered films against the Si substrate. The effective thickness was regarded as the sum of the Al thickness and the cap metal thickness. The effective stress was calculated from the curvature of the Si substrate according to Eq. (1),

$$\sigma=\frac{E}{6(1-\nu)}\frac{t_s^2}{t_f}\frac{1}{R'}, \tag{1}$$

where σ = effective layered film stress, E = Young's modulus of Si substrate, ν = Poisson's ratio of Si substrate, t_f = total thickness of layered film, t_s = thickness of Si substrate, and R = curvature radius of Si substrate.

The composition and structure for the bilayer metal films were characterized by x-ray diffraction analysis (XRD).

 0021-8979/92/140958-08$04.00

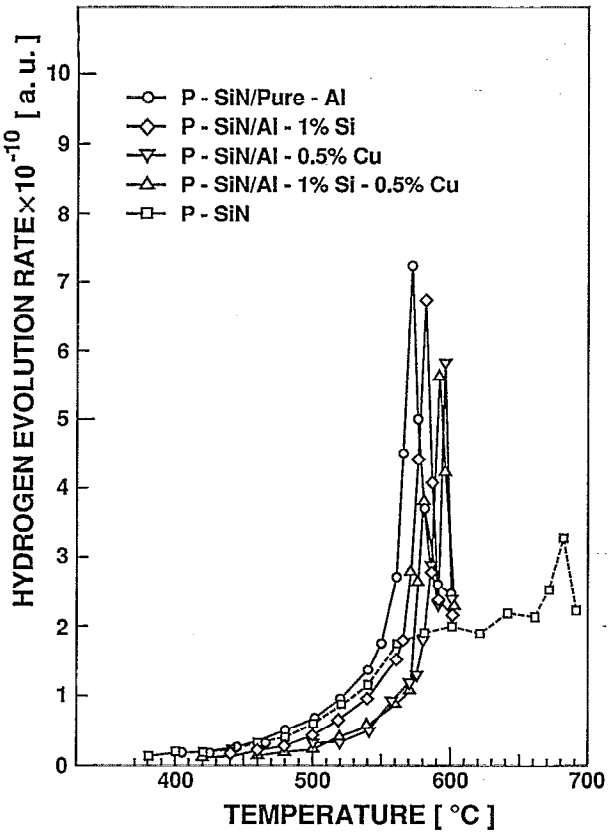

FIG. 1. Hydrogen evolution rates as a function of annealing temperature for the *P*-SiN films deposited on pure-Al, Al-1%Si, Al-0.5%Cu, and Al-1%Si-0.5%Cu films as well as on a Si substrate.

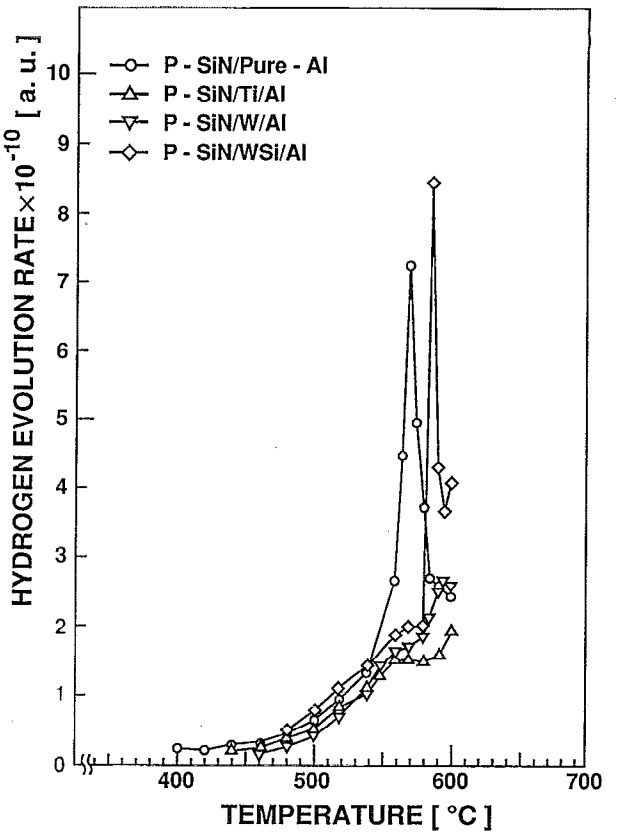

FIG. 2. Hydrogen evolution rates as a function of annealing temperature for the *P*-SiN films deposited on pure-Al, Ti-capped Al, W-capped Al, and WSi_x-capped Al films.

III. RESULTS

The dependence of underlying Al-alloys on hydrogen evolution from *P*-SiN films was investigated. Hydrogen evolution rates versus annealing temperatures for the *P*-SiN films, which were deposited on a Si substrate and Al-alloys, such as pure-Al, Al-1%Si, Al-0.5%Cu, and Al-1%Si-0.5%Cu, are shown in Fig. 1. The hydrogen evolution rates increased with increasing annealing temperatures. Sharp peaks in hydrogen evolution rates were observed for the *P*-SiN films on Al-alloys, whereas no peaks were observed for the *P*-SiN film on a Si-substrate except for a small peak at 680 °C, which was due to the decomposition of H_2O in the vacuum. The sharp peak indicated a burst of hydrogen molecules due to crack formation in the *P*-SiN film blisters,[8] in which hydrogen molecules accumulated.[8] The degree of the influence of the underlying metals appeared in the peak temperature for the hydrogen evolution rate. Hydrogen evolution rate peak temperatures for the *P*-SiN films deposited on pure-Al, Al-1%Si, Al-0.5%Cu, and Al-1%Si-0.5%Cu films, were 570, 580, 595, and 580/590 °C, respectively, It should be noted that the hydrogen evolution rate for the *P*-SiN film on Al-1%Si-0.5%Cu had two peaks: 580 and 590 °C. They may be related to the peaks for both Al-1%Si, 580 °C, and Al-0.5%Cu, 595 °C, respectively. The reason why Al-Si and Al-Si-Cu films have the same peak temperature, 580 °C, for the hydrogen evolution rates is due to the same characteristics of the films in terms of temperature. The eutectic temperatures for bulk Al-Si and Al-Cu are 577 and 548 °C, respectively.[14] However, bulk Al-1 wt.%Si begins to melt, that is, both liquid and solid phases are formed, at approximately 600 °C, while Al-0.5 wt.%Cu begins to melt at approximately 660 °C, which is close to the melting point for bulk pure-Al. Therefore, the 1%Si addition to Al-0.5%Cu reduces the melting point so that Al-1%Si and Al-1%Si-0.5%Cu have the same peak temperature at 580 °C due to Si addition. The difference in the measured peak temperature, 580 °C, and the bulk melting point from the literature, 600 °C, may be attributed to lowering the melting point due to thin film effect and to uneven distribution of Si concentration.

The *P*-SiN film on Al-0.5%Cu showed the highest peak temperature for the hydrogen evolution rate. Therefore, Cu addition to the underlying Al film suppressed the hydrogen evolution from the *P*-SiN film and raised the hydrogen evolution peak temperature. On the other hand, the Si addition to the Al-0.5%Cu film reduced the hydrogen evolution rate peak temperature for the cover *P*-SiN film from 595 to 580 °C.

Hydrogen evolution rates versus annealing temperatures for the *P*-SiN films deposited on the pure-Al, Ti-capped Al, W-capped Al, and WSi-capped Al films, are shown in Fig. 2. The refractory metal capping on an underlying Al layer raised the peak temperature for the hy-

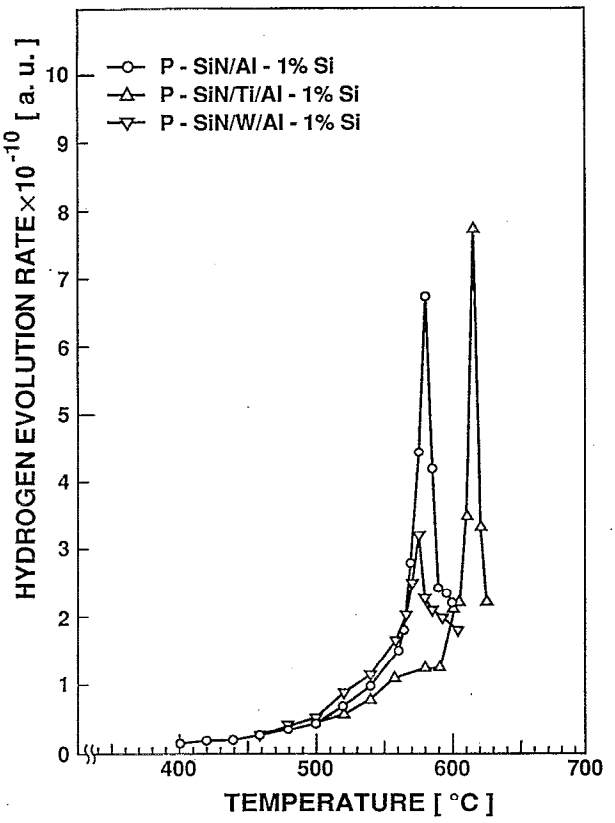

FIG. 3. Hydrogen evolution rates as a function of annealing temperature for the *P*-SiN films deposited on Al-1%Si, Ti-capped Al-1%Si, and W-capped Al-1%Si films.

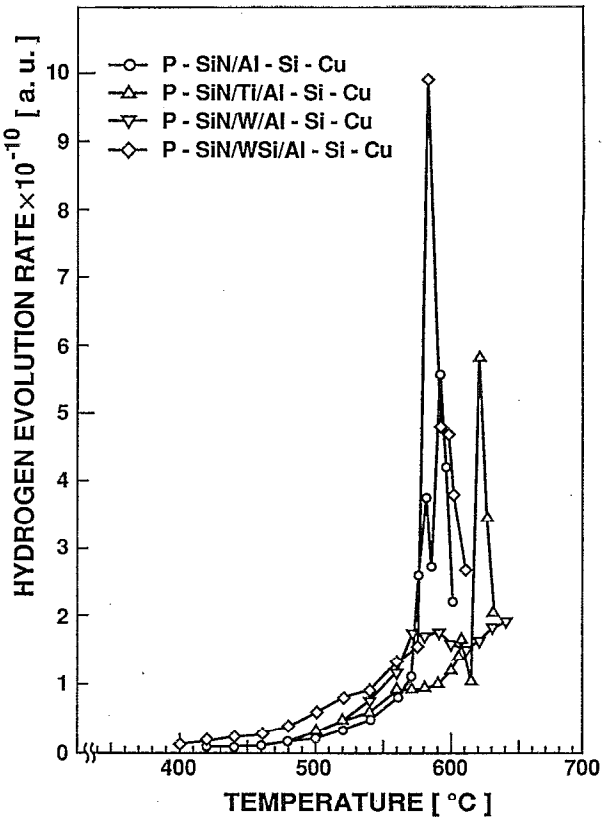

FIG. 4. Hydrogen evolution rates as a function of annealing temperature for the *P*-SiN films deposited on Al-1%Si-0.5%Cu, Ti-capped Al-1%Si-0.5%Cu, W-capped Al-1%Si-0.5%Cu, and WSi_x-capped Al-1%Si-0.5%Cu films.

drogen evolution rate for the *P*-SiN films on Al. Neither Ti-capped Al nor W-capped Al showed any peaks, except for a small peak at 595 °C for the W-capped Al. Therefore, Ti-capping on the underlying Al could raise the hydrogen evolution peak temperature for the cover *P*-SiN film. The peak temperature for the *P*-SiN film on WSi_x-capped Al was 585 °C, which was close to that for the *P*-SiN on Al-1%Si, shown in Fig. 1.

Hydrogen evolution rates versus annealing temperatures for the *P*-SiN films, deposited on the Al-1%Si, Ti-capped Al-1%Si, and W-capped Al-1%Si films, are shown in Fig. 3. The peak temperatures for W-capped Al-1%Si and Al-1%Si without a cap layer were 575 and 580 °C, respectively. On the other hand, Ti-capped Al-1%Si showed the highest peak temperature, 615 °C. Consequently, Ti-capping on Al-1%Si also raised the hydrogen evolution rate peak temperature for the cover *P*-SiN film.

Hydrogen evolution rates versus annealing temperatures for the *P*-SiN films deposited on the Al-1%Si-0.5%Cu, Ti-capped Al-1%Si-0.5%Cu, W-capped Al-1%Si-0.5%Cu and WSi_x-capped Al-1%Si-0.5%Cu films are shown in Fig. 4. The peak temperatures for the *P*-SiN films on Al-1%Si-0.5%Cu, WSi_x/Al-1%Si-0.5%Cu and Ti/Al-1%Si-0.5%Cu were 580, 585, and 620 °C, respectively. Small peaks were observed for the *P*-SiN film on W/Al-1%Si-0.5%Cu at 570 and 590 °C. Again, the Ti-capped Al-1%Si-0.5%Cu film showed the highest peak temperature for the hydrogen evolution rate, i.e., 620 °C.

The results shown in Figs. 2–4 are summarized in Table I. It was found that the Ti-capping on the Al-alloys raised the hydrogen evolution rate peak temperature for the cover *P*-SiN films approximately 30 to 40 °C, in comparison with Al-alloys without cap layers, while W and WSi_x cappings did not show any appreciable increase in the peak temperature.

IV. DISCUSSION

A. Dependence of underlying Al-alloys on hydrogen evolution

Figure 5 shows the hydrogen evolution rate as a function of reciprocal temperature for the *P*-SiN films on Al-alloys and a Si-substrate. At less than approximately

TABLE I. Hydrogen evolution rate peak temperatures for *P*-SiN films deposited on various metal layers.

Underlying metal	Without cap layer	Ti-cap	W-cap	WSi-cap
Pure-Al	570 °C	> 600 °C	595 °C	585 °C
Al-1%Si	580 °C	615 °C	575 °C	...
Al-0.5%Cu	595 °C	...	...	...
Al-1%Si-0.5%Cu	580/590 °C	620 °C	570 °C	580 °C

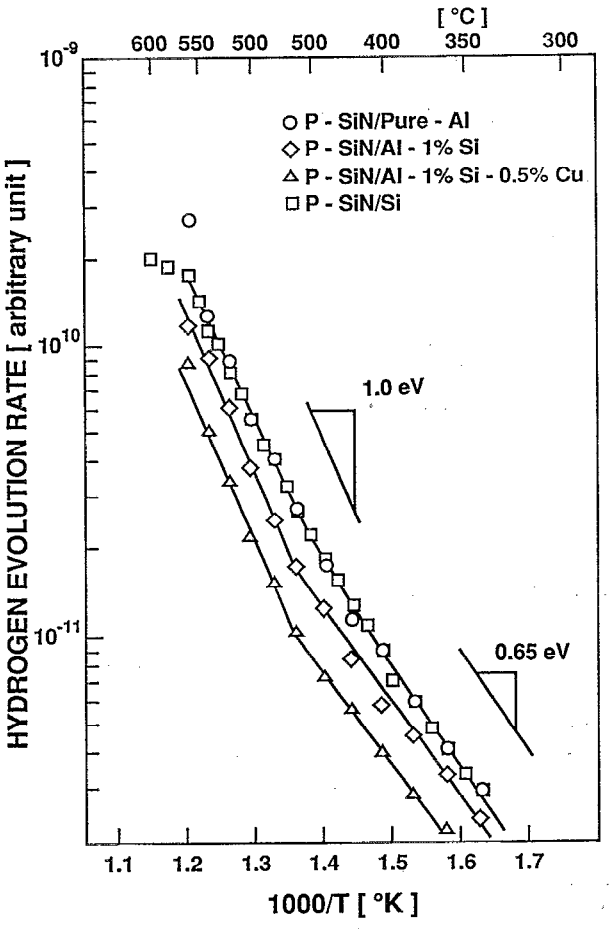

FIG. 5. Hydrogen evolution rate as a function of reciprocal temperature for *P*-SiN films deposited on Al-alloys and a Si substrate.

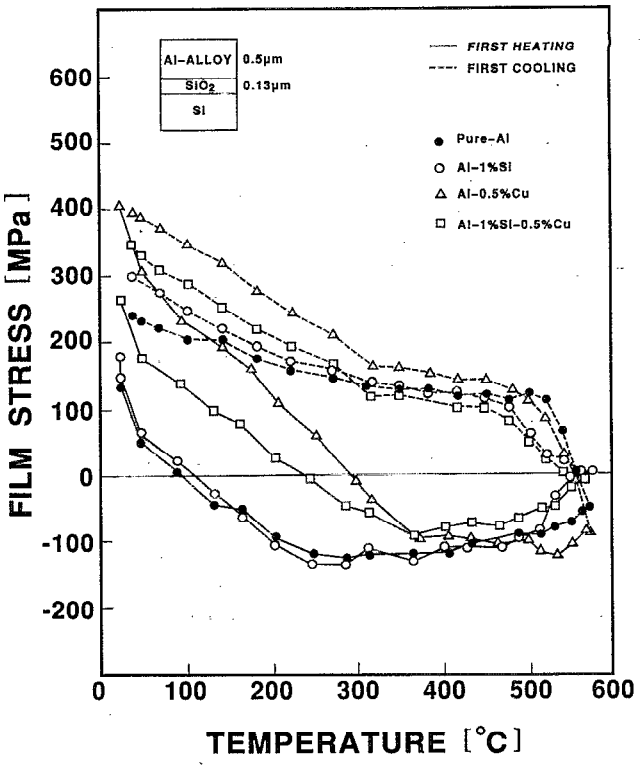

FIG. 6. Film stresses as a function of annealing temperature for pure-Al, Al-1%Si, Al-0.5%Cu, and Al-1%Si-0.5%Cu films deposited on oxidized Si substrates.

550 °C, the hydrogen evolution rates for the *P*-SiN films on Al-alloys, in terms of temperatures, increased exponentially. The slopes in terms of reciprocal temperature were not dependent on underlying materials. The slope for the *P*-SiN film on Al was the same as that for the *P*-SiN film on Si, which is correlated to the activation energy for hydrogen evolution from the *P*-SiN film. At less than approximately 450 °C, the slope was 0.65 ± 0.05 eV and at more than approximately 450 °C, the slope was 1.0 ± 0.05 eV. Although the reason for the difference in the slope is not clear, the hydrogen evolution could be attributed to the hydrogen desorption from the *P*-SiN film. In addition, the difference in the intensity of the hydrogen evolution rate, which is equivalent to the difference in the detected current by the quadrupole mass spectrometer, may be caused by the difference in the sample volume.

On the other hand, above 550 °C, the hydrogen evolution rates were strongly dependent on the underlying materials as shown in Figs. 2–4. The sources of the hydrogen may be attributed to the decomposition of N—H bonds, as well as the desorption of hydrogen molecules from the *P*-SiN films.[9] During heat treatments, some of desorbed hydrogen molecules accumulated at the interface between the *P*-SiN film and underlying Al film, resulting in the formation of the *P*-SiN film blisters. The blisters may also be formed due to both *P*-SiN film adhesion loss from the softened Al during heat treatment and *P*-SiN film intrinsic stress change.

In order to study the influences of underlying Al-alloys, thermal and mechanical properties of the underlying Al-alloys were investigated. Figure 6 shows mechanical stresses for pure-Al, Al-1%Si, Al-0.5%Cu, and Al-1%Si-0.5%Cu films as a function of annealing temperature. In the temperature versus stress curves, six regions were apparent.[15]

The first region on heating showed the elastic behavior. Tensile stresses for pure-Al and Al-1%Si films decreased linearly, due to the thermal expansion coefficient mismatch between the Al film and the Si-substrate, and turned to compressive stress as temperature increased from room temperature to 240 °C. The elastic regions for Al-0.5%Cu and Al-1%Si-0.5%Cu films were from room temperature to 360 °C. Both the Al-1%Si-0.5%Cu and Al-0.5%Cu films showed a wider temperature range for the elastic behavior than pure-Al and Al-1%Si films. This is due to the hardening effect by Cu addition and the intermetallic compound formation, such as $CuAl_2$, at grain boundaries.

In the second region on heating, plastic deformation occurred. The slopes of the stress versus temperature curves became zero and the stress remained constant in the temperature ranges from 240 to 500 °C for pure-Al and Al-1%Si films, and from 360 to 500 °C for Al-1%Si-0.5%Cu and Al-0.5%Cu films. The constant stress indicated the compressive yield strength, approximately — 100

MPa. This is due to the stress relaxation as well as to softening, recrystallization, and grain growth of the Al films. Hillock formation in the Al films also occurred to relieve the compressive stress in these temperature ranges because the compressive stress, due to the thermal expansion mismatch, exceeded the yield strength.

In the third region above 500 °C, the stresses in the Al films in which Si was added, such as Al-1%Si and Al-1%Si-0.5%Cu, reached zero. This is due to the fact that the Si addition to Al bulks reduces the melting point from 660 to 577 °C at which both liquid and solid phases exist.[14] For Al thin films, the melting point further reduces in comparison with Al bulks.

During cooling, the compressive stresses reduced linearly and turned to tensile stress in the fourth region from 550 to 450 °C. In this region, the elastic deformation occurred.

In the fifth region, from 450 to 300 °C the tensile film stress became constant, approximately + 150 MPa, which was the yield tensile strength. Plastic deformations, such as voiding and dislocations in the Al film, occurred in this region.

In the sixth region, below 300 °C, elastic behavior was observed again, especially for Al-Cu alloys. Copper addition to the Al film made the residual tensile stress greater than that for the Al without Cu addition. Furthermore, the slopes of the stress versus temperature curves for Al films with Cu addition were steeper than those without Cu addition. This is due to the hardening effect of the $CuAl_2$ precipitation at the grain boundaries.

Therefore, Cu addition to the Al film improved thermal properties of the Al film, such as hardening and plastic deformation suppression due to the grain boundary precipitation of $CuAl_2$. On the other hand, the Si addition to the Al film softened the films at a higher temperature range, above 550 °C as a result of lowering the melting point from 660 to approximately 600 °C, at which both liquid and solid phases existed for Al-1%Si bulk.[14]

Consequently, the higher peak temperature for the hydrogen evolution rate for the *P*-SiN film on the Al-0.5%Cu film could be attributed to the suppression of plastic deformation in the underlying Al film, due to the hardening effect. On the other hand, the lower peak temperature of the hydrogen evolution rate for the *P*-SiN film on the Al-1%Si-0.5%Cu film was attributed to the lower melting point, due to the Si addition in the Al-0.5%Cu film.

B. Dependence of underlying bilayer metals on hydrogen evolution

Since the sharp peak in the hydrogen evolution rate is attributed to the crack formation in the *P*-SiN film blister in which hydrogen molecules accumulated,[8] it is necessary for underlying metals to suppress the *P*-SiN film blister formation. Titanium capping on Al could suppress the hydrogen evolution by suppressing *P*-SiN film blister crack formation because the effects of Ti-capping on Al are to prevent adhesion loss of the *P*-SiN film and to form a hard and thermally stable intermetallic compound on the Al film surface.

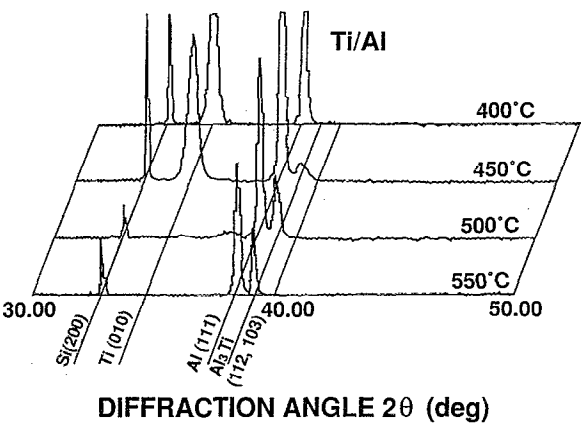

FIG. 7. X-ray diffraction patterns for Ti-capped Al films annealed at 400, 450, 500, and 550 °C, respectively.

Figure 7 shows typical XRD patterns for Ti/Al layered films annealed at 400, 450, 500, and 550 °C, respectively. An intermetallic compound $TiAl_3$(112,103) was formed after annealing at 450 °C, while the Ti(010) cap layer still existed. Since the Ti(010) peak disappeared after 500 °C annealing, Ti turned to $TiAl_3$. The intermetallic compound $TiAl_3$ has a high melting point, 1340 °C,[14] and is more than 40 times harder than Al in Vickers hardness.[16]

Figure 8 shows typical XRD patterns for W/Al layered films annealed at 400, 450, 500, and 550 °C, respectively. No intermetallic compound was formed after 450 °C annealing. Intermetallic compounds WAl_{12}(310,321) were formed after 500 °C annealing. After 550 °C annealing, WAl_{12}(222,400) and WAl_5(110,112) were formed. The W film may cause the *P*-SiN film blister due to the adhesion loss of the *P*-SiN film from the W surface because the W surface is less adhesive than the Al surface.

Figure 9 shows typical XRD patterns for WSi_x/Al layered films annealed at 400, 450, 500, and 550 °C, respectively. The silicon-rich tungsten silicide film was amorphous after annealing at 400 °C because no peaks for WSi_2

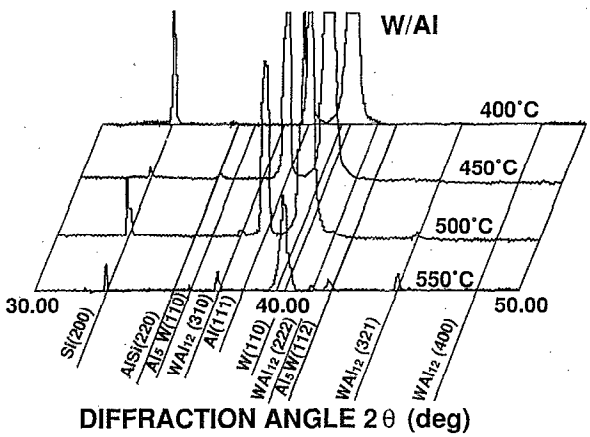

FIG. 8. X-ray diffraction patterns for W-capped Al films annealed at 400, 450, 500, and 550 °C, respectively.

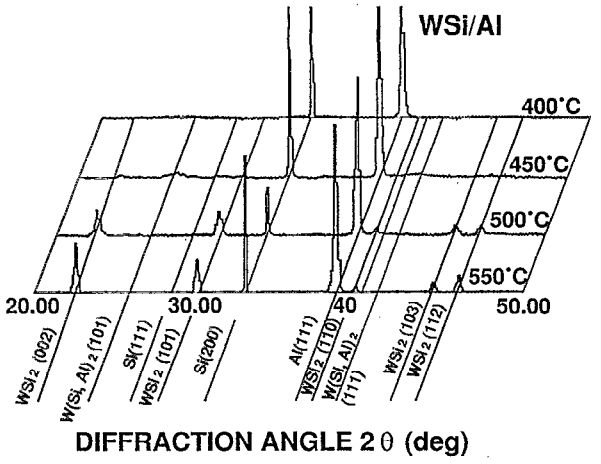

FIG. 9. X-ray diffraction patterns for WSi_x-capped Al films annealed at 400, 450, 500, and 550 °C, respectively.

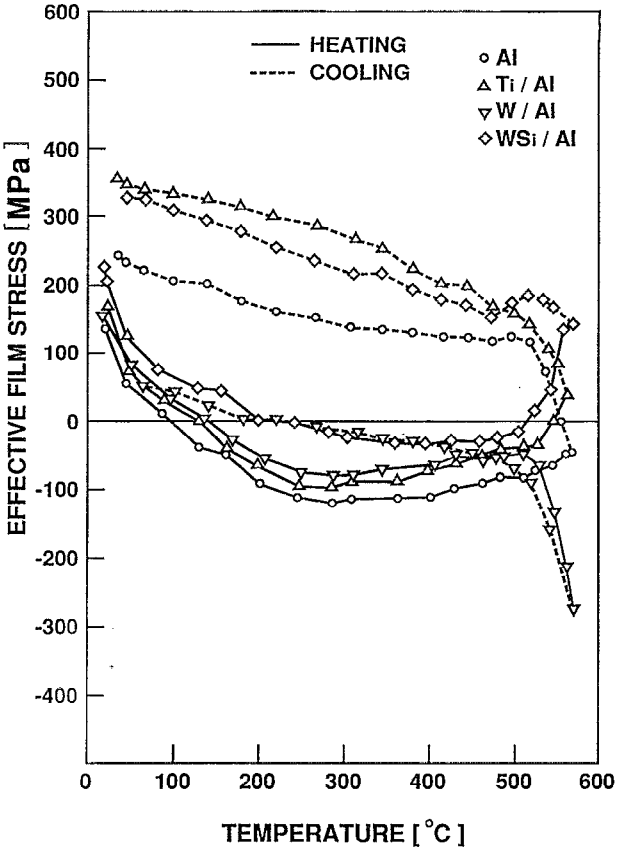

FIG. 10. Effective layered film stresses as a function of annealing temperature for pure-Al, Ti-capped Al, W-capped Al, and WSi_x-capped Al films deposited on oxidized Si substrates.

were observed. Broad hexagonal $W(Si,Al)_2(111,101)$ peaks were observed after 450 °C annealing. Hexagonal WSi_2 may also be formed. Tetragonal $WSi_2(002,101,110,111,103,112)$ peaks were observed and hexagonal $W(Si,Al)_2$ or hexagonal WSi_2 peaks disappeared after 500 °C annealing. Interdiffusions of Si, W, and Al occurred at above 450 °C.[17] The Si diffusion into Al lowered the melting point for the Al. The interdiffusions also caused both WSi_x/Al bilayer thickness reduction and surface morphology degradation, resulting in *P*-SiN film blister formation.

Figure 10 shows effective layered film stresses as a function of annealing temperature for pure-Al, Ti-capped Al, W-capped Al, and WSi_x-capped Al films deposited on oxidized Si substrates, corresponding to the results shown in Fig. 2. Figure 11 shows effective layered film stresses as a function of annealing temperature for Al-1%Si, Ti-capped Al-1%Si, and W-capped Al-1%Si films deposited on oxidized Si substrates, corresponding to the results shown in Fig. 3. Figure 12 shows effective layered film stresses as a function of annealing temperature for Al-1%Si-0.5%Cu, Ti-capped Al-1%Si-0.5%Cu, W-capped Al-1%Si-0.5%Cu and WSi_x-capped Al-1%Si-0.5%Cu films deposited on oxidized Si substrates, corresponding to the results shown in Fig. 4.

During heating from room temperature to 450 °C, effective stress behaviors in terms of annealing temperatures for the various layered films were similar. These results indicated that the stress behavior of the underlying Al film was dominant in the effective stress calculations for layered metals below 450 °C, although Young's modulus for the cap metals and a silicide were different and larger than that for Al. This is due to the fact that no significant reaction occurred below 450 °C between cap metals and Al. These results also correspond to the fact that the hydrogen evolution rates versus temperature curves were similar for the *P*-SiN films on the various layered metal films in the temperature range below 450 °C, as shown in Figs. 3–5.

On the other hand, above 450 °C, effective stresses for the various layered films, i.e., curvatures of the Si substrates, changed differently. The effective stresses for the WSi_x/Al and Ti/Al bilayers changed toward the tensile direction, while that for the W/Al bilayer changed toward the compressive direction, as shown in Fig. 10. The molar volume of Al, W, WAl_{12}, and WAl_5 are 9.995, 9.5, 10.09×13, and 9.25×6 cm^3/mole, respectively.[15] The formation of WAl_{12} causes volume increase, while the formation of WAl_5 causes volume reduction. The volume increase by the formation of WAl_{12} causes negative (compressive) stress change of 454 MPa assuming that all of Al turns to WAl_{12} homogeneously and causes only volume expansion resulting in the 0.4% linear expansion. However, measured stress change was approximately 250 MPa, which was smaller than the calculated value. Therefore, the formation of WAl_5 compensated for the part of the negative stress change due to the volume reduction. The negative (compressive) stress change of the intermetallic compound could suppress the *P*-SiN film blister formation because the negative warp of the Si substrate could match the intrinsic stress in the *P*-SiN film. Consequently, the lower peak temperature for the hydrogen evolution rate for the *P*-SiN film on W/Al-alloy could be attributed to the adhesion loss of the cover *P*-SiN film from the W film surface. The lower hydrogen evolution rates, at the peak temperatures for the *P*-SiN films on W/Al-alloys, might be attributed to the fewer *P*-SiN blister formations as a result of the negative (compressive) stress change in the bilayer.

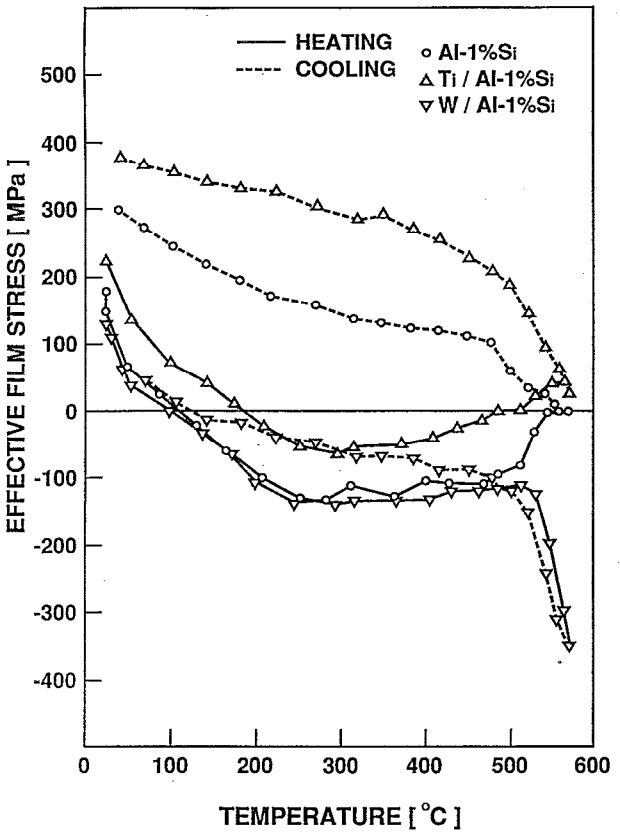

FIG. 11. Effective layered film stresses as a function of annealing temperature for Al-1%Si, Ti-capped Al-1%Si, and W-capped Al-1%Si films deposited on oxidized Si substrates.

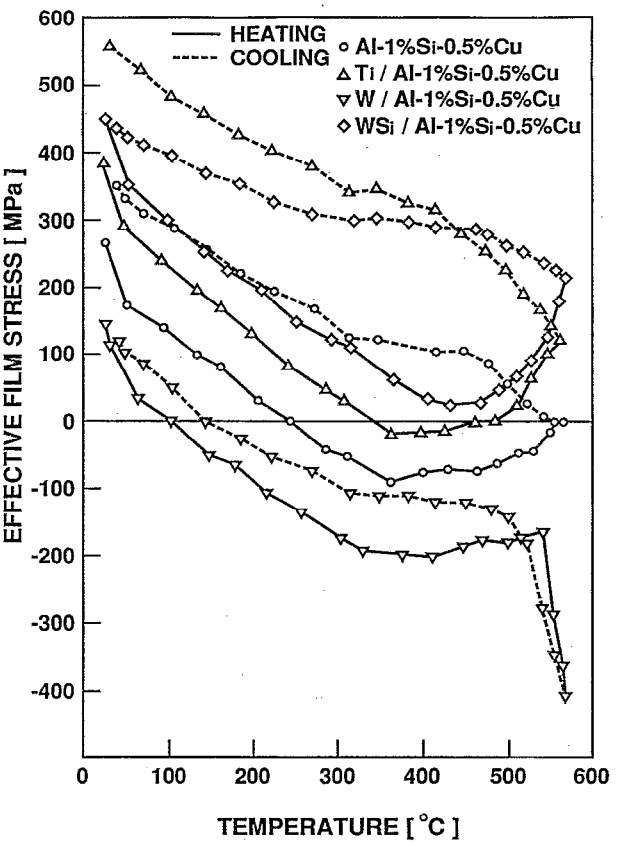

FIG. 12. Effective layered film stresses as a function of annealing temperature for Al-1%Si-0.5%Cu, Ti-capped Al-1%Si-0.5%Cu, W-capped Al-1%Si-0.5%Cu, and WSi_x-capped Al-1%Si-0.5%Cu films deposited on oxidized Si substrates.

The effective stress change toward the tensile direction for the WSi_x/Al bilayer was more noticeable than that for the Ti/Al bilayer. However, the lowest hydrogen evolution peak temperature for the WSi_x/Al bilayer and the highest peak temperature for the Ti/Al bilayer, shown in Fig. 2, could not be explained merely by the results of the effective film stresses for the layered films shown in Fig. 10. Therefore, the lowest peak temperature for the hydrogen evolution for the WSi_x/Al, compared with those for Ti/Al and W/Al, could be attributed to the adhesion loss of the cover *P*-SiN film as results of both surface morphology degradation and softening of Al film due to Si diffusion. Figure 11 showed results similar to those shown in Fig. 10, except for the zero stress above 550 °C due to the formation of both liquid and solid phases for the Al-Si alloy.[14]

The results, shown in Fig. 12, indicated that the Ti/Al-1%Si-0.5%Cu layered film did not show a plateau in the tensile stress, during cooling from 550 °C. It is indicated that little plastic deformation occurred in the Ti/Al-1%Si-0.5%Cu bilayer after the heat treatment. Consequently, the highest hydrogen evolution peak temperature for the *P*-SiN film on Ti/Al-1%Si-0.5%Cu could be attributed to both the least plastic deformation of the underlying bilayer and the Ti adhesive layer, resulting in the suppression of the *P*-SiN blister crack formation.

V. CONCLUSION

The influence of underlying metals on hydrogen evolution from *P*-SiN films was investigated. The hydrogen evolution rates for the *P*-SiN films on Al-alloys and cap-metal/Al-alloy bilayers increased as annealing temperature increased and sharp peaks in the hydrogen evolution rates were observed.

Copper addition to the Al film raised the hydrogen evolution peak temperature for the *P*-SiN film, while Si addition to the Al-Cu alloy reduced the peak temperature. Titanium capping on the Al-alloys also raised the hydrogen evolution rate peak temperature for the *P*-SiN films.

Consequently, the hydrogen evolution from the *P*-SiN film could be suppressed either by depositing the Ti cap layer on the underlying Al film or by adding Cu to the Al film.

ACKNOWLEDGMENTS

The authors thank Dr. M. Ohta and Dr. M. Ogawa for their encouragement, and Dr. S. Okuda for film stress simulation.

[1] J. Curry, G. Fitzgibbon, Y. Guan, R. Muollo, G. Nelson, and A. Thomas, *Proceedings of the 22nd International Reliability Physics Symposium* (IEEE, New York, 1984), p. 6.

[2]J. T. Yue, W. P. Funsten, and R. V. Taylor, *Proceedings of the 23rd International Reliability Physics Symposium* (IEEE, New York, 1985), p. 126.
[3]J. W. McPherson and C. F. Dunn, J. Vac. Sci. Technol. B **5**, 1321 (1987).
[4]K. Hinode, N. Owada, T. Nishioka, and K. Mukai, J. Vac. Sci. Technol. B **5**, 518 (1987).
[5]T. Turner and K. Wendel, *Proceedings of the 23rd International Reliability Physics Symposium* (IEEE, New York, 1985), p. 142.
[6]J. Klema, R. Pyle, and E. Domangue, *Proceedings of the 22nd International Reliability Physics Symposium* (IEEE, New York, 1984), p. 1.
[7]R. A. Gasser, Jr. and S. G. Johnson, J. Vac. Sci. Technol. B **4**, 758 (1986).
[8]T. Kikkawa, H. Watanabe, and T. Murata, Appl. Phys. Lett. **50**, 1527 (1987).
[9]T. Kikkawa and H. Watanabe, *Abstracts of the Electronic Materials Conference* (TMS, Warrendale, PA, 1989), p. 17.
[10]H. Koyama, Y. Mashiko, and T. Hishioka, *Proceedings of the 24th International Reliability Physics Symposium* (IEEE, New York, 1986), p. 24.
[11]T. Kikkawa, N. Endo, K. Yamazaki, and H. Watanabe, *Proceedings of the VLSI Multilevel Interconnection Conference* (IEEE, New York, 1989), p. 463.
[12]K. Hinode, I. Asano, and Y. Homma, IEEE Trans. Electron Devices **36**, 1050 (1989).
[13]K. Tokunaga and K. Sugawara, J. Electrochem. Soc. **138**, 176 (1991).
[14]M. Hansen, *Constitution of Binary Alloys* (McGraw-Hill, New York, 1958).
[15]D. S. Gardner, Ph.D. dissertation, Stanford University, 1988.
[16]G. V. Samsonov and I. M. Viniskii, *Handbook of Refractory Compounds* (IFI/Plenum Data Company, New York, 1980).
[17]T. Kikkawa and N. Endo, J. Appl. Phys. **70**, 2370 (1991).